Canadian Journal of Forest Research

Article

Assessing the influence of simulated ice storm-induced crown damage on nonstructural carbohydrates, wound closure, and radial growth of maple trees

Paul G. Schaberg[a], **Christopher F. Hansen**[b], **Paula F. Murakami**[a], **Gary J. Hawley**[b], **John L. Campbell**[c], **and Lindsey E. Rustad**[c]

[a]Northern Research Station, Forest Service, US Department of Agriculture, Burlington, VT 05405, USA; [b]Rubenstein School of the Environment and Natural Resources, University of Vermont, Burlington, VT 05405, USA; [c]Northern Research Station, Forest Service, US Department of Agriculture, Durham, NH 03824, USA

Corresponding author: **Paul G. Schaberg** (email: paul.schaberg@usda.gov)

Abstract

We evaluated shoot nonstructural carbohydrate (NSC) concentrations, stem wound closure, and radial growth of sugar maple (*Acer saccharum* Marsh.) and red maple (*Acer rubrum* L.) trees in a novel ice storm experiment in which five storm treatments (0, 6.4, 12.7, and 19.1 mm of radial ice accretion in 1 year and 12.7 mm of ice in two consecutive years) were applied within a mature northern hardwood forest. We tested for changes in physiology at two levels: (1) associated with plot-level ice treatments and (2) with crown damage classes of individual trees. Few differences in NSC or wound closure associated with treatment were found. Growth decreased for red maple in the medium and high treatments and sugar maple in the high treatment but no other treatments. Changes in physiology were more evident when assessed using crown damage classes. Two NSC components were elevated in sugar and red maples with high (≥50%) crown damage. Wound closure was less for red maples with high damage, and separation among damage classes was even greater for sugar maple. Red maples with moderate (<50%) and high crown damage showed gradually declining growth, whereas sugar maples with high damage showed ∼80% reduction in growth the first year after injury.

Key words: red maple, sugar maple, basal area increment, tree rings, sugars and starch concentrations

Introduction

The frequency and intensity of severe weather events are projected to increase with climate change (Wuebbles et al. 2014; IPCC CC 2014), and there is a need for information about the short- and long-term impacts of these events, especially as they relate to forest systems. Ice storms are an example of a severe weather event that is a major driver of forest disturbance in temperate and boreal systems worldwide (e.g., Ding et al. 2009; Rustad and Campbell 2012; Nagel et al. 2016). Climate models suggest that ice storms will become more frequent and intense with climate change (e.g., Cheng et al. 2011; Swaminathan et al. 2018), which means that their influence on forests could become more consequential. The ice loading that occurs during ice storms can remove fine shoots, break off branches, and even snap main trunks or topple trees (Irland 2000; Rhoads et al. 2002). However, the influence of this loss of woody tissue on tree function after the ice load melts has received little experimental evaluation.

Most knowledge of the influence of ice storm damage on tree structure and function comes from post facto studies that evaluate the aftereffects of naturally occurring ice storms (Irland 2000; Rhoads et al. 2002; Smith and Shortle 2003). These studies have generally shown that ice damage can cover vast land areas but are often patchy in disturbance intensity and damage (Irland 2000). For example, in January 1998, an ice storm of long duration (approximately 1 week; DeGaetano 2000) and significant magnitude of ice loading (some locations receiving over 10 cm of radial ice accumulation) damaged trees across more than 10 000 000 hectares of forest in the northeastern United States and adjacent Canada (Ireland 1998). Although extensive in area impacted, damage to forests varied considerably across the region. Factors such as latitude (e.g., ice loading was generally greater in the north; DeGaetano 2000), local topography (elevation and aspect; Millward and Kraft 2004), and forest composition (hardwoods were generally damaged more than conifers; Irland 1998; Millward and Kraft 2004) influenced the nature and extent of initial damage to forests. Among hardwood species, sugar maple (*Acer saccharum* Marsh.) and red maple (*Acer rubrum* L.) were often reported as being widely damaged (Irland 1998; Hooper et al. 2001), with crown injury associated with near-term (3 year) reductions in radial growth (Smith and Shortle 2003). Post facto studies also suggest that the loss of above ground woody shoots and branches from ice damage can alter concentrations of nonstructural carbohydrates (NSC; sugars plus starch) in residual shoots (Wong et al. 2005) and reduce wound closure on trees (Shortle et al. 2003), presumably as NSC are removed with lost branches or shunted elsewhere to rebuild crowns. To our knowledge, no study has made an integrated evaluation of the influence of ice damage on multiple carbon-related tree parameters (e.g., NSC, wound closure, and radial growth) at one time.

Because of the stochastic spatial and temporal occurrence of ice storms, post facto studies, although informative, often have deficient pre-storm forest inventory data for establishing baseline conditions, lack true experimental undamaged control stands for comparisons, and seldom include immediate post-storm impact assessments (Rustad et al. 2020). To overcome these limitations, methodologies were recently developed to generate simulated ice storms whereby a gradient of ice loads could be replicated in forest plots to experimentally test how the amount and frequency of ice accumulation can alter a range of forest parameters (Campbell et al. 2020; Rustad et al. 2020). These methods were used to create the first replicated, simulated ice storm experiment (ISE) that enabled evaluation of the influence of ice amount (0, 6.4, 12.7, and 19.1 mm of ice accumulation on branches—levels that approximated National Weather Service ice storm warning levels or an extreme ice event such as occurred in 1998 (Rhoads et al. 2002)) and ice frequency (for the 12.7 mm treatment—1 and 2 years of treatment) on canopy structure (Fahey et al. 2020) and nitrogen dynamics (Weitzman et al. 2020) within a northern hardwood forest. Here, we extend these evaluations to also include the influence of experimental ice loading on three measures of tree carbon relations: (1) shoot NSC, (2) closure of wounds on the main stems, and (3) radial basal area growth of dominant and co-dominant sugar maple and red maple trees on experimental plots. We hypothesized that increased crown damage with greater ice accumulation would:

- H^1 lead to small increases in short-term NSC in remaining shoots as less carbon was diverted to close wounds (H^2) or grow stems (H^3),
- H^2 be associated with reduced wound closure because carbon stores that fuel callose formation would be depleted when shoots and branches were shed or used to rebuild crowns, and
- H^3 the overall disruption of tree carbon reserves would result in reduced radial growth.

Materials and methods

Ice treatments

This study was conducted as part of the ISE, which was initiated in 2015 at the Hubbard Brook Experimental Forest (HBEF) in the southern part of the White Mountain National Forest (43°56′N, 71°45′W) in New Hampshire, USA. The climate at HBEF is considered cold continental, with mean January temperatures of −9 °C, mean July temperatures of 18 °C, and the mean annual precipitation being ∼1400 mm. The ISE was established in a 70–100-year-old mixed-hardwood forest dominated by sugar maple (*A. saccharum*), red maple (*A. rubrum*), yellow birch (*Betula alleghaniensis* Britton), and American beech (*Fagus grandifolia* Ehrh.) trees.

For details of the experimental approach and methods of creating simulated ice storm treatments, see Rustad et al. (2020) and Campbell et al. (2020). Briefly, 10 20 m × 30 m plots were established—two per each of five treatments with differing levels and frequency of ice addition: (1) Control, no experimental icing (0 mm ice), (2) Low, 6.4 mm ice in year 1 only, (3) Mid, 12.7 mm of ice in year 1 only, (4) Midx2, 12.7 mm of ice in years 1 and 2, and (5) High, 19.1 mm of ice in year 1 only. Targeted levels of ice loading were chosen to reflect National Weather Service Ice Storm Warnings for the northeastern, USA: 6.4 mm in the mid-Atlantic region and 12.7 mm for New York and New England. Whereas the High treatment approximated ice levels from an extreme event such as occurred in the region in 1998 (Rhoads et al. 2002). Ice treatments were established under subfreezing conditions across five dates in year 1 (2016) and one date in year 2 (2017).

Ice treatment levels were verified using calipers to measure ice accretion on four wooden dowel "ornaments" suspended within forest canopies in each treatment plot (Campbell et al. 2020; Rustad et al. 2020). Accretion levels were significantly different among the treatments and were close to target levels (typically within 2 mm except for the high treatment, which was within 5 mm; Fahey et al. 2020). Experimental ice loading resulted in crown damage and loss that was measured as increased fine and coarse woody debris on the ground (Rustad et al. 2020), decreased leaf area, and increased gaps and structural irregularities within canopies (Fahey et al. 2020). It was expected that progressive branch loss with increased ice loading would result in treatment-specific averages in damage that could influence the tree-based measures related to our three hypotheses. However, because there was sometimes considerable variation in crown injury within treatments and plots (Rustad et al. 2020), we also visually assessed the relative crown loss within individual trees for which we measured shoot NSC, wound closure, and radial growth. Crown damage was rated into three classes: (1) no visible damage, (2) moderate damage (<50% crown loss), and (3) high damage (≥50% crown loss).

Although ISE plots overall contained a mix of tree species, only sugar and red maple trees were abundant enough to allow for replicated measurements of NSC, wound closure, and radial growth across treatment plots. The same sugar maple and red maple trees from dominant and co-dominant crown classes were used to assess all physiological traits. The average diameter at breast height (DBH) of sugar maple trees at the time of their last sampling was 32.4 (±1.71 SE) cm and their average age was 104.1 (±0.58) years. The average DBH of red maple trees at the time of their last sampling was 35.7 (±2.22) cm and their average age was 105.3 (±1.26) years. There were no significant differences in size (P = 0.2414) or age (P = 0.3682) between the species.

NSC analyses

In early August of 2016 and 2017, woody shoots were removed from tree canopies using shotguns and were transported on ice to the laboratory where they were stored at

−20 °C prior to chemical analysis. The quantification of soluble sugars and starch followed the methods of Wong et al. (2005). The bark, phloem, and pith were removed from small segments (approximately 1 cm) of each twig. The remaining xylem tissue was submerged in individual 5 mL vials containing 80% ethanol. Vials were then placed in a boiling water bath and vacuum infiltrated at −52 kPa. Woody tissue was macerated in 80% ethanol using a Polytron™ (Brinkman Instruments, Westbury, NY), centrifuged at 3000 rpm in glass test tubes for 15 min, and subsequently extracted two times in an 80 °C water bath. After each extraction, the supernatant was poured into a new centrifuge tube and the final volume of ethanol extract was recorded. The remaining pellet was air dried at room temperature.

For the analysis of individual soluble sugars, each sample supernatant was passed through a 0.45 μm filter into a 250 μL limited volume insert and then oven-dried at 37 °C. Once dried, sugar samples were re-constituted in 200 μL Ca-EDTA solvent (0.05 g/L) and analyzed for stachyose, raffinose, sucrose, glucose, xylose, and fructose using a Waters Alliance HPLC system (Milford, MA) and a Waters Sugar-Pak column (0.1 $mmol^{-1}$ Ca EDTA at 90 °C). Individual sugars were identified via a Waters 2414 refractive index detector using known standards, quantified, and expressed as mg g^{-1} of oven-dried tissue. For determination of starch, the dried pellet was gelatinized with 0.2 N KOH in a boiling water bath for 30 min, neutralized with 1.0 mol/L acetic acid and hydrolyzed to glucose using amyloglucosidase (Sigma 10115). Glucose was detected using a glucose hexokinase kit (Pointe Scientific, Canton, MI) and a Bio-Tek Instruments ELx800 UV microplate reader (Winooski, VT) at 340 nm. Glucose standard curves were used to calculate starch concentration (expressed as mg g^{-1} dry tissue).

Stem wounding and wound closure

In November 2015, sugar maple and red maple trees on all treatment plots were wounded using a 25 mm cork borer that removed bark tissues down to the active bark cambium on the east and west sides of the main trunks of trees at DBH (1.37 m above ground level). The inside diameter of wounds was measured with a caliper to the nearest 0.1 mm in September 2021 to determine the extent of callus formation and wound closure among trees and treatments. This measurement was then subtracted from the initial wound diameter (i.e., 25 mm) to represent the amount of wound closure.

Radial growth

Collection of increment cores began in October of 2019 and concluded in November of 2020 due to the logistical constraints of the COVID-19 pandemic. All dominant and co-dominant red maple and sugar maple trees on each of the eight treatment and two control plots were sampled following standard dendrochronological techniques (Stokes and Smiley 1968); two xylem increment cores were collected per tree (180° from each other) at DBH and perpendicular to the predominant slope. Cores were air dried, mounted on wooden blocks, and sanded with progressively finer sandpaper.

The list method (Yamaguchi 1991) was used to visually crossdate annual tree-ring increments, which were then microscopically measured to 0.001 mm resolution with a Velmex sliding stage unit (Velmex, Inc., Bloomfield, New York) and Measure J2X software (v.5.05, VoorTech Consulting, Holderness, New Hampshire). The program COFECHA (v6.06p) was used to statistically detect and subsequently correct crossdating errors, as well as calculate chronology statistics (e.g., series intercorrelation, average mean sensitivity, and autocorrelation; Bunn et al. 2013). Tree age at breast height was recorded for each core when pith was present and estimated using a pith indicator (Speer 2010) for cores where pith was not present but showed curvature of the inner most rings.

Annual tree-ring increments were averaged for the two cores per tree, and basal area increment (BAI) was calculated to standardize and assess general tree growth. BAI converts diameter increments (cm/year) to area increments (cm^2/year) to reduce size- and age-related growth trends (Cook and Kairiukstis 1990). BAI chronologies were calculated for each species regardless of plot and within each plot by species. A ratio of pre-treatment BAI growth (5-year baseline average) to each year of post-treatment growth was calculated to assess the potential impact of the ISE treatments.

Statistical analyses

Variations in shoot NSC, wound closure, and radial growth were assessed at two levels: (1) differences associated with simulated ice storm treatments and (2) differences associated with crown damage classes post treatment for individual sample trees. Analyses of Variance (ANOVAs) and Wilcoxon non-parametric tests were used to test for differences in measurement parameters using JMP Pro 15 statistical software (SAS Institute, Inc, Cary, NC). Differences among specific means were assessed using a Tukey's HSD post-hoc test for parametric data, and a Steel–Dwass test for non-parametric data. Statistical tests were considered significant if $P \leq 0.05$. For BAI growth, slopes of the linear relationship of growth over time were calculated for each treatment category and tested to assess whether they were significantly different from zero (significant negative slopes indicated post-treatment growth declines). To test for specific year-to-year differences in BAI for trees within a treatment or crown damage class category, ANOVAs were combined with orthogonal contrasts to identify when significant changes in post-treatment growth occurred.

Results

Treatment differences in NSC, wound closure, and BAI growth

There were very few significant differences in the concentrations of shoot NSCs associated with ice treatment, and for the rare differences that were detected, patterns did not match treatment intensities. For red maples in 2016, concentrations of total sugars were higher in shoots in the Mid treatment relative to Control and High treatments (Table 1). Whereas in 2017, there was a tendency for total NSC (sugars

 Can. J. For. Res. **54:** 512–523 (2024) | dx.doi.org/10.1139/cjfr-2023-0119

Table 1. Nonstructural carbohydrate means (±1 SE) across ice treatments for dominant and co-dominant red maple trees in 2016 and 2017.

	2016					
Red maple	Control	Low	Mid	Mid × 2	High	Prob > *F*
Starch (mg/g)	24.9 ± 6.50	16.1 ± 0.00	32.2 ± 10.5	40.7 ± 2.20	31.6 ± 2.80	0.4410
Stachyose (mg/g)	0.10 ± 0.04	0.11 ± 0.00	0.17 ± 0.08	0.08 ± 0.06	0.11 ± 0.06	0.8726
Raffinose (mg/g)	0.37 ± 0.08	0.50 ± 0.00	0.63 ± 0.18	0.42 ± 0.14	0.42 ± 0.12	0.6999
Sucrose (mg/g)	5.01 ± 0.70	5.69 ± 0.00	8.28 ± 1.13	5.38 ± 0.07	4.93 ± 0.93	0.1149
Glucose (mg/g)	0.29 ± 0.10	0.31 ± 0.00	0.44 ± 0.06	0.38 ± 0.18	0.28 ± 0.11	0.8592
Xylose (mg/g)	2.50 ± 0.28	1.39 ± 0.00	3.51 ± 0.74	2.19 ± 0.35	2.45 ± 0.37	0.2639
Fructose (mg/g)	0.50 ± 0.12	0.42 ± 0.00	0.53 ± 0.08	0.64 ± 0.21	0.39 ± 0.08	0.6811
Total sugar (mg/g)	8.76 ± 0.54^{B}	8.42 ± 0.00^{B}	13.6 ± 1.33^{A}	9.08 ± 1.00^{AB}	8.58 ± 1.08^{B}	**0.0272**
Total NSC (mg/g)	33.7 ± **6.97**	24.5 ± **0.00**	45.8 ± **10.6**	49.8 ± **2.90**	40.2 ± **3.60**	0.**4018**
	2017					
Red maple	Control	Low	Mid	Mid x 2	High	Prob > F
Starch (mg/g)	23.1 ± **4.40**	14.8 ± **0.00**	29.6 ± **3.80**	19.9 ± **2.40**	22.1 ± **2.80**	0.**3001**
Stachyose (mg/g)	0.18 ± **0.05**	0.05 ± **0.00**	0.14 ± **0.03**	0.14 ± **0.03**	0.20 ± **0.07**	0.**7701**
Raffinose (mg/g)	0.94 ± **0.14**	0.67 ± **0.00**	1.19 ± **0.26**	0.98 ± **0.18**	1.00 ± **0.19**	0.**8392**
Sucrose (mg/g)	7.44 ± **1.21**	5.82 ± **0.00**	13.5 ± **2.97**	8.96 ± **1.11**	8.26 ± **1.20**	0.**1212**
Glucose (mg/g)	2.76 ± **0.29**	1.57 ± **0.00**	4.19 ± **0.96**	3.09 ± **0.19**	3.12 ± **0.57**	0.**2835**
Xylose (mg/g)	4.36 ± **0.56**	2.24 ± **0.00**	4.82 ± **0.64**	4.70 ± **0.86**	4.86 ± **1.08**	0.**8036**
Fructose (mg/g)	2.30 ± **0.34**	1.34 ± **0.00**	3.65 ± **0.74**	2.80 ± **0.30**	3.19 ± **0.65**	0.**3336**
Total sugar (mg/g)	17.9 ± **1.19**	11.7 ± **0.00**	27.5 ± **4.98**	20.7 ± **1.89**	20.6 ± **3.04**	0.**1722**
Total NSC (mg/g)	41.1 ± **4.91**^{A}	26.5 ± **0.00**^{B}	57.1 ± **3.95**^{A}	40.5 ± **1.87**^{A}	42.7 ± **4.88**^{A}	**0**.0398

Note: Means with different uppercase letters are significantly different based on Tukey's HSD tests ($P \leq 0.05$). Concentrations represent constituent mass per unit dry tissue mass.

plus starch) to be lower in red maple in the Low treatment than trees in the other treatments, although the post-hoc Tukey's HSD test could not distinguish which specific treatments differed from one another (Table 1). For sugar maple in 2016, shoot sucrose concentrations in trees in the Midx2 treatment were lower than trees in the Low treatment, and total sugars in the Midx2 were lower than in trees in the Low treatment (Table 2). There were no treatment-associated differences in shoot NSC detected for sugar maples in 2017 (Table 2).

Similar to findings for NSC, few differences in wound closure associated with ice treatments were detected. For red maple, no differences in wound closure in 2021 (6 years after initial wounding in 2015) were found (Table 3). For sugar maple, significant differences associated with treatment were detected, although the post-hoc Tukey's HSD test could not distinguish which specific treatments differed from one another (Table 3). In general, for sugar maples in 2021, there was a tendency for trees in the Low and High treatments to show the least wound closure.

Radial growth measurement of red maple and sugar maple trees showed a gradual increase in BAI growth as forests matured in the early-to-mid 1900s and exhibited modest growth thereafter that varied from year-to-year. Whereas growth for red maples plateaued at about 9 cm^2 right up to treatment initiation, growth for sugar maples peaked at roughly 13 cm^2, but then steeply declined starting in the 1980s (Fig. 1). To evaluate the influence of treatment on the growth of trees, we calculated BAI post treatment relative to the average growth for each tree for 5 years pre-treatment. For red maple, this relative growth showed some separation in growth in at least 2 years post treatment (Fig. 2). Here, the most consistent pattern was that red maple in the Midx2 and High treatments were growing less than trees in the Low treatment. We also analyzed whether the slope of growth over time post treatment was significantly different from zero (e.g., if treatment initiated a decline in growth). For red maple, this analysis showed that growth significantly decreased over time for trees in the Mid, Midx2, and High treatments but did not decline for trees in the Control or Low treatments (Table 4). For sugar maple, no differences in relative growth among trees attributable to treatments was found overall (Fig. 3), and slope analysis detected reductions in growth over time solely for trees in the High treatment (Table 4).

Differences in NSC, wound closure, and BAI growth among crown damage classes

Because there was sometimes considerable variation in crown damage among trees within treatment plots, we also evaluated differences in NSC, wound closure, and BAI growth based on the post-treatment crown damage ratings of individual trees.

There were extremely few differences in NSC among trees in the three crown damage rating groups. For red maple in 2016, there were no differences in starch, any of the six individual sugars, total sugar, or total NSC associated with crown damage class (Table 5). For red maple in 2017, there were no differences associated with crown damage class in any of the

Table 2. Nonstructural carbohydrate means (±1 SE) across ice treatments of dominant and co-dominant sugar maple trees in 2016 and 2017.

	2016					
Sugar maple	Control	Low	Mid	Mid × 2	High	Prob > *F*
Starch (mg/g)	20.3 ± 1.40	23.1 ± 3.60	31.6 ± 0.00	22.3 ± 3.30	19.5 ± 1.90	0.6633
Stachyose (mg/g)	0.01 ± 0.00	0.02 ± 0.01	0.01 ± 0.00	0.02 ± 0.01	0.01 ± 0.0	0.8864
Raffinose (mg/g)	0.38 ± 0.07	0.49 ± 0.04	0.40 ± 0.00	0.33 ± 0.06	0.38 ± 0.05	0.3553
Sucrose (mg/g)	10.8 ± 1.49^{AB}	12.4 ± 1.04^{A}	14.1 ± 0.00^{AB}	7.40 ± 1.21^{B}	10.0 ± 0.88^{AB}	**0**.0400
Glucose (mg/g)	0.64 ± 0.13	0.68 ± 0.05	0.79 ± 0.00	0.46 ± 0.10	0.79 ± 0.11	0.2184
Xylose (mg/g)	2.17 ± 0.23	2.87 ± 0.29	2.78 ± 0.00	2.07 ± 0.34	2.83 ± 0.31	0.2166
Fructose (mg/g)	0.63 ± 0.09	0.63 ± 0.06	0.70 ± 0.00	0.48 ± 0.08	0.77 ± 0.10	0.2225
Total sugar (mg/g)	14.6 ± 1.78^{AB}	17.1 ± 1.25^{A}	18.8 ± 0.00^{AB}	10.8 ± 1.46^{B}	14.8 ± 1.15^{AB}	**0**.0339
Total NSC (mg/g)	34.9 ± 2.22	40.1 ± 4.69	50.4 ± 0.00	33.0 ± 3.85	34.3 ± 2.04	0.3933
	2017					
Sugar maple	Control	Low	Mid	Mid x 2	High	Prob > F
Starch (mg/g)	20.3 ± 1.30	20.3 ± 2.00	13.5 ± 8.90	20.5 ± 2.20	22.4 ± 2.50	0.5466
Stachyose (mg/g)	0.01 ± 0.01	0.08 ± 0.05	0.01 ± 0.01	0.09 ± 0.05	0.03 ± 0.01	0.4615
Raffinose (mg/g)	0.77 ± 0.11	1.22 ± 0.19	0.52 ± 0.52	1.20 ± 0.26	0.75 ± 0.14	0.1499
Sucrose (mg/g)	11.4 ± 1.44	14.3 ± 0.89	8.24 ± 8.11	12.8 ± 2.41	9.90 ± 1.69	0.3361
Glucose (mg/g)	3.75 ± 0.45	5.03 ± 0.54	2.31 ± 1.26	4.10 ± 0.46	4.47 ± 0.54	0.1599
Xylose (mg/g)	2.84 ± 0.45	3.87 ± 0.42	2.09 ± 0.65	3.58 ± 0.62	3.25 ± 0.47	0.4039
Fructose (mg/g)	3.08 ± 0.42	3.67 ± 0.46	2.20 ± 0.41	2.80 ± 0.29	3.60 ± 0.46	0.3789
Total sugar (mg/g)	21.8 ± 2.58	28.1 ± 1.90	15.4 ± 11.0	24.5 ± 3.86	22.0 ± 2.78	0.2749
Total NSC (mg/g)	42.1 ± 3.15	48.4 ± 2.98	28.9 ± 19.9	45.0 ± 4.36	44.4 ± 4.56	0.3399

Note: Means with different uppercase letters are significantly different based on Tukey's HSD tests ($P \leq 0.05$). Concentrations represent constituent mass per unit dry tissue mass.

Table 3. Wound closure growth by treatment (mm; mean ± SE) for red maple and sugar maple trees measured in 2021.

	Treatment					
Species	Control	Low	Mid	Mid × 2	High	Prob > *F*
Red maple	12.07 ± 2.92	8.19 ± 0	10.58 ± 3.55	6.79 ± 5.89	11.30 ± 2.93	0.8744
Sugar maple	12.70 ± 1.98^{A}	7.93 ± 3.97^{A}	18.92 ± 1.06^{A}	16.92 ± 0.37^{A}	7.94 ± 1.09^{A}	**0.0410**

Note: Means with different uppercase letters are significantly different based on Tukey's HSD tests ($P \leq 0.05$).

Fig. 1. Average basal area increment (BAI) growth for red maple and sugar maple trees on ISE plots at the Hubbard Brook Experimental Forest. The first year of treatment (2016) and the number of trees measured per species are noted.

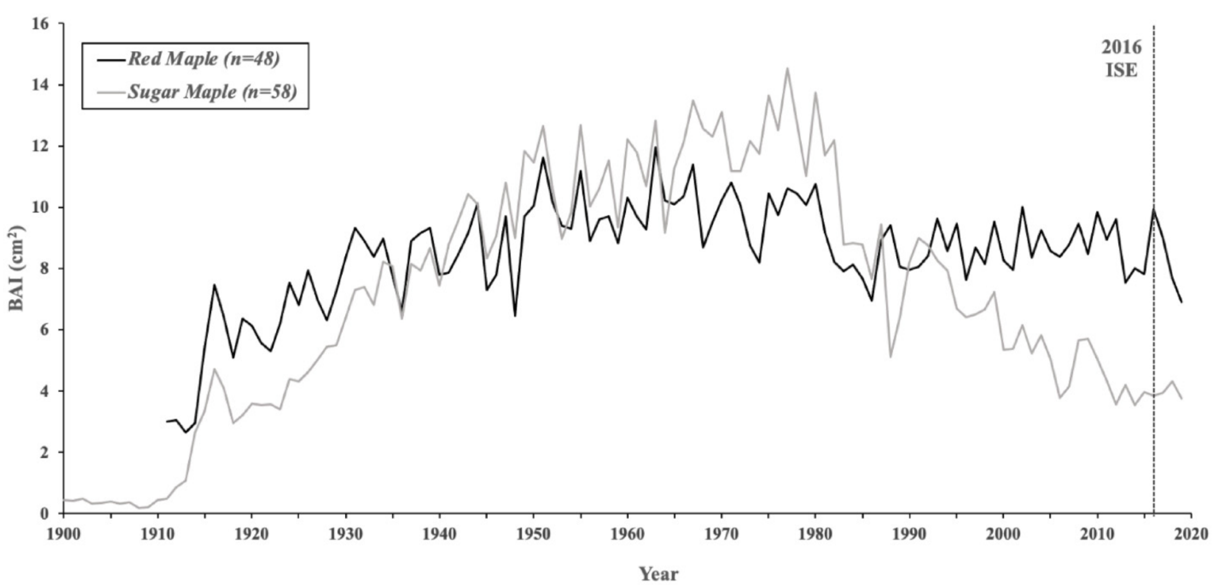

Fig. 2. Basal area increment (BAI) growth relative to 5-year average growth before the first year of treatment (2016) for red maple trees on plots that received one of five ice load treatments: Control, Low, Mid, Midx2, and High. The number of plots measured per treatment are noted. Means with different uppercase letters are significantly different based on Tukey's HSD tests ($P \leq 0.05$); NS indicates that no statistical differences were detected. Error bars represent ±SE.

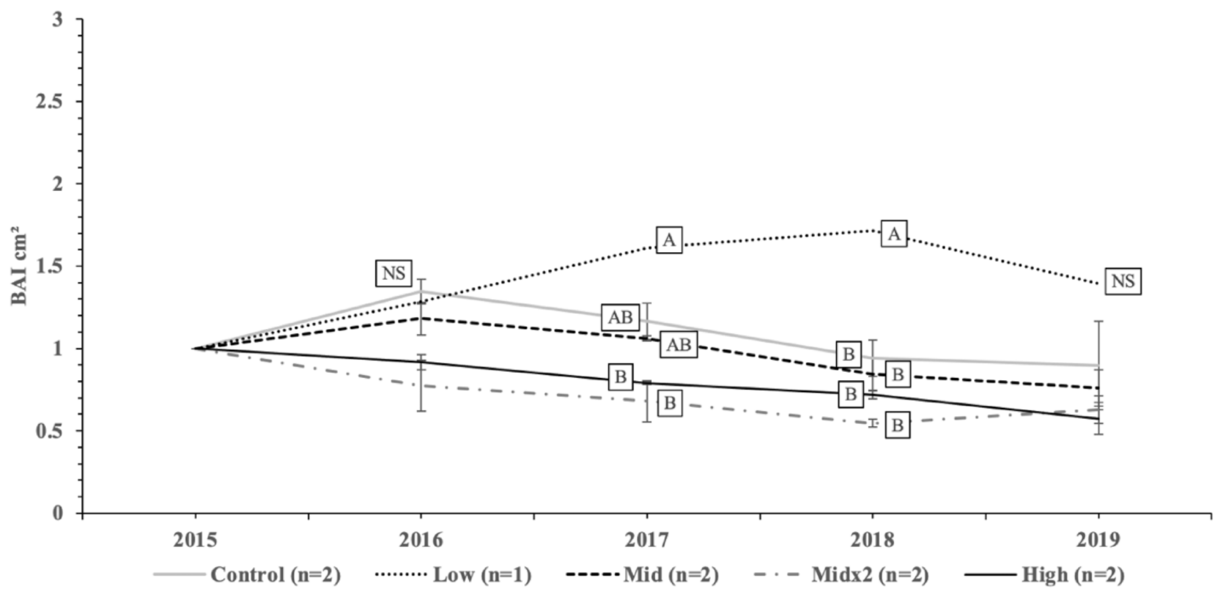

Table 4. Analysis of regression line slopes of relative BAI growth over time post treatment for red maple and sugar maple trees in ISE plots.

Species	Treatment	*N*	Slope	Std. err.	Prob > *F* (sig. from zero)	R^2
Red maple	Control	2	− 0.0614	±0.072	0.2550	0.1582
	Low	1	0.1213	–	0.2037	0.4666
	Mid	2	− 0.0819	±0.042	**0.0319**	0.4570
	Midx2	2	− 0.0970	±0.001	**0.0127**	0.5609
	High	2	− 0.1047	±0.017	**<0.0001**	0.8903
	Prob > *F*	–	0.1718	–	–	–
Sugar maple	Control	2	0.0118	±0.032	0.8003	0.0085
	Low	2	0.0793	±0.126	0.7335	0.0153
	Mid	2	0.0070	±0.019	0.9204	0.0013
	Midx2	2	0.0088	±0.010	0.8444	0.0051
	High	2	− 0.1302	±0.055	**0.0120**	0.5666
	Prob > *F*	–	0.3447	–	–	–

Note: Whether treatment-specific slopes are significantly different from zero are noted as *P* values in bold (negative slopes indicate significant growth declines post treatment).

NSC categories except one—concentrations of stachyose were higher in trees with 50% or greater crown damage relative to trees with lesser crown damage (Table 5). For sugar maples in 2016, there were no differences in any component or composite NSC measure except for xylose, which was higher in trees with 50% or greater crown damage relative to trees with lesser crown damage (Table 6). No differences in NSC were found for sugar maple in 2017 (Table 6).

Differences in wound closure among the crown damage categories more closely matched a priori expectations of reduced wound closure with greater crown damage. For red maple, wound closure for trees that had high crown damage or were eventually rated as dead was generally less than trees rated as having less crown damage (Table 7). For sugar maple, the pattern was even more evident; trees with no or moderate crown damage had more wound closure than trees with high crown damage, which had more wound closure than trees eventually rated as dead (Table 7).

ANOVA analyses found no differences in relative BAI growth for either red maple (Fig. 4) or sugar maple (Fig. 5) associated with the three crown damage classes. However, tests of the slopes of regression lines for relative BAI growth over time showed that for red maple trees in the moderate and high crown damage categories, growth gradually declined over time post ice treatment (Table 8). Red maple with no crown damage showed no decline in growth post treatment. For sugar maple trees with no or moderate crown damage, no declines in growth were detected (regression line

Fig. 3. Basal area increment (BAI) growth relative to 5-year average growth before the first year of treatment (2016) for sugar maple trees on plots that received one of five ice load treatments: Control, Low, Mid, Midx2, and High. The number of plots measured per treatment are noted. NS indicates that no statistical differences were detected. Error bars represent ±SE.

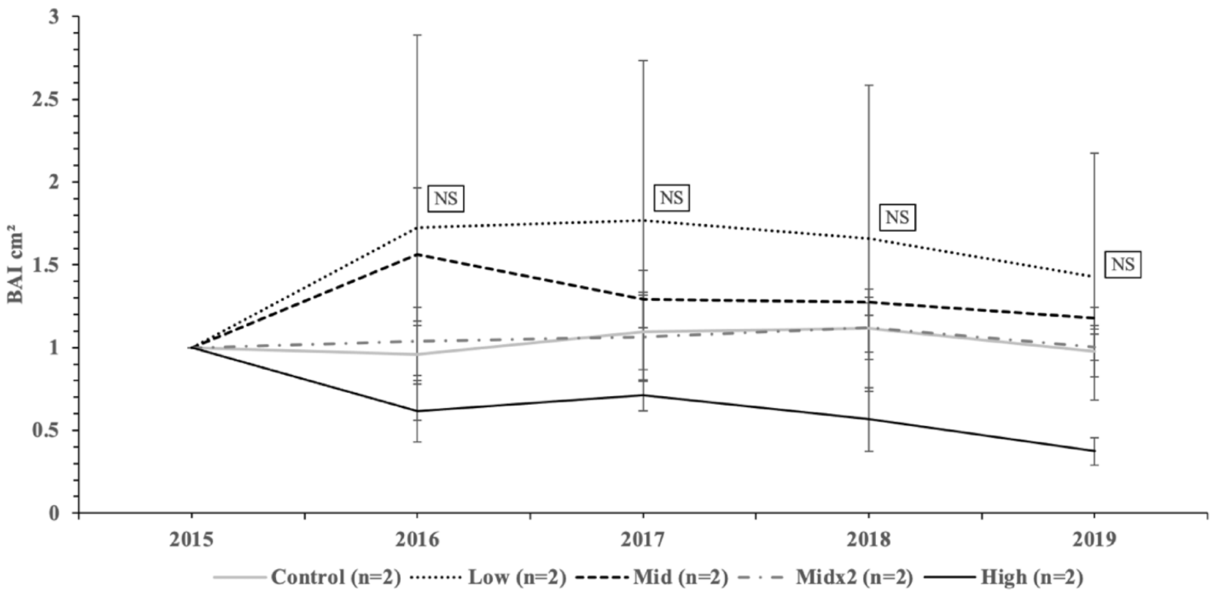

Table 5. Nonstructural carbohydrate means (±1 SE) across crown damage classes of dominant and co-dominant red maple trees in 2016 and 2017.

	2016			
Red maple	No damage	<50%	≥50%	Prob > *F*
Starch (mg/g)	28.0 ± 4.31	33.5 ± 4.80	28.5 ± 0.00	0.6947
Stachyose (mg/g)	0.06 ± 0.03	0.16 ± 0.05	0.16 ± 0.00	0.2023
Raffinose (mg/g)	0.34 ± 0.07	0.58 ± 0.10	0.40 ± 0.00	0.1578
Sucrose (mg/g)	5.01 ± 0.47	6.71 ± 0.84	3.98 ± 0.00	0.1750
Glucose (mg/g)	0.24 ± 0.07	0.40 ± 0.07	0.51 ± 0.00	0.2286
Xylose (mg/g)	2.29 ± 0.26	2.90 ± 0.40	2.47 ± 0.00	0.4617
Fructose (mg/g)	0.45 ± 0.09	0.52 ± 0.07	0.56 ± 0.00	0.7811
Total sugar (mg/g)	8.40 ± 0.40	11.3 ± 1.12	8.09 ± 0.00	0.0704
Total NSC (mg/g)	36.4 ± 4.50	44.7 ± 5.05	36.6 ± 0.00	0.4675
	2017			
Red maple	No damage	<50%	≥50%	Prob > *F*
Starch (mg/g)	23.0 ± 1.54	22.3 ± 1.88	30.1 ± 0.00	0.6477
Stachyose (mg/g)	0.11 ± 0.01^{B}	0.15 ± 0.02^{B}	0.52 ± 0.00^{A}	**0.0008**
Raffinose (mg/g)	0.77 ± 0.19	1.00 ± 0.10	1.52 ± 0.00	0.3512
Sucrose (mg/g)	6.83 ± 1.88	9.29 ± 0.94	10.4 ± 0.00	0.6817
Glucose (mg/g)	2.52 ± 0.20	3.26 ± 0.29	2.38 ± 0.00	0.6005
Xylose (mg/g)	4.03 ± 0.21	4.63 ± 0.47	4.57 ± 0.00	0.9204
Fructose (mg/g)	2.00 ± 0.47	3.00 ± 0.29	2.47 ± 0.00	0.5312
Total sugar (mg/g)	16.3 ± 1.18	21.3 ± 1.68	21.9 ± 0.00	0.6337
Total NSC (mg/g)	39.2 ± 0.36	43.6 ± 2.70	51.9 ± 0.00	0.6702

Note: Means with different uppercase letters are significantly different based on Tukey's HSD tests ($P \leq 0.05$). Concentrations represent constituent mass per unit dry tissue mass.

slopes were not significantly different from zero). Although the slope of the regression of growth over time for sugar maple with moderate crown damage was negative (suggesting a growth slowdown), this slope was not significantly different from zero—indicating that no linear association between crown damage and radial growth was evident. However, orthogonal contrasts of growth over time showed that there was a significant ($P = 0.02$) reduction in BAI between 2015 (pre-treatment) and 2016 (the first-year post treatment) for sugar maples with high crown damage, and that growth

Table 6. Nonstructural carbohydrate means (±1 SE) across crown damage classes of dominant and co-dominant sugar maple trees in 2016 and 2017.

	2016			
Sugar maple	No damage	<50%	≥50%	Prob > *F*
Starch (mg/g)	19.7 ± 1.24	23.6 ± 2.34	18.4 ± 4.71	0.3190
Stachyose (mg/g)	0.01 ± 0.01	0.01 ± 0.00	0.01 ± 0.00	0.9885
Raffinose (mg/g)	0.41 ± 0.05	0.39 ± 0.04	0.38 ± 0.14	0.8981
Sucrose (mg/g)	10.7 ± 0.84	9.98 ± 0.97	9.95 ± 2.48	0.8447
Glucose (mg/g)	0.67 ± 0.07	0.64 ± 0.07	0.52 ± 0.22	0.7496
Xylose (mg/g)	2.20 ± 0.17^{B}	2.57 ± 0.23^{AB}	3.84 ± 0.51^{A}	**0.0207**
Fructose (mg/g)	0.63 ± 0.07	0.65 ± 0.06	0.44 ± 0.15	0.4487
Total sugar (mg/g)	14.7 ± 1.03	14.2 ± 1.18	15.1 ± 3.42	0.9410
Total NSC (mg/g)	34.4 ± 1.51	37.8 ± 3.08	33.5 ± 6.83	0.5953
	2017			
Sugar maple	No damage	<50%	≥50%	Prob > *F*
Starch (mg/g)	21.4 ± 2.79	19.9 ± 1.04	26.8 ± 11.4	0.3339
Stachyose (mg/g)	0.01 ± 0.00	0.06 ± 0.02	0.01 ± 0.01	0.5937
Raffinose (mg/g)	0.66 ± 0.10	0.99 ± 0.11	1.04 ± 0.36	0.5652
Sucrose (mg/g)	12.2 ± 1.83	11.8 ± 0.95	13.2 ± 5.81	0.9352
Glucose (mg/g)	4.31 ± 0.62	4.15 ± 0.29	5.84 ± 0.13	0.3563
Xylose (mg/g)	2.98 ± 0.60	3.26 ± 0.26	5.04 ± 0.84	0.2166
Fructose (mg/g)	3.63 ± 0.54	3.09 ± 0.22	5.08 ± 0.18	0.0768
Total sugar (mg/g)	23.8 ± 2.80	23.3 ± 1.62	30.2 ± 5.02	0.5776
Total NSC (mg/g)	45.2 ± 4.63	43.3 ± 2.11	57.0 ± 16.4	0.3141

Note: Means with different uppercase lettera are significantly different based on Tukey's HSD tests ($P \leq 0.05$). Concentrations represent constituent mass per unit dry tissue mass.

Table 7. Wound closure growth by treatment (mm; mean ± SE) measured in 2021 for red maple and sugar maple trees among crown damage classes.

	Damage class				
Species	No damage	<50%	≥50%	Dead	Prob > *F*
Red maple	13.35 ± 2.93^{AB}	11.20 ± 1.10^{A}	5.19 ± 0.97^{BC}	1.58 ± 1.44^{C}	**0.0005***
Sugar maple	18.70 ± 1.07^{A}	13.45 ± 0.98^{B}	5.56 ± 1.53^{C}	0.27 ± 0.20^{D}	**<0.0001***

*Means with different uppercase letters are significantly different based on non-parametric Wilcoxon/Kruskal–Wallis test—differences among damage classes determined by Steel–Dwass test.

remained at this low level thereafter. Indeed, reductions in radial growth were more immediate and dramatic for sugar maple (approximately −80%) within the highest crown damage category compared to red maple (approximately −30%) with this level of injury.t

Discussion

ISE treatments

We hypothesized that increasing canopy damage with the advancing magnitude or frequency of ISE treatments would result in increased NSC in the short term and reduced wound closure and BAI growth thereafter. However, when data were analyzed as plot means across the replicated five treatments, there was little evidence of treatment effects that were consistent with progressive crown damage.

Concentrations of NSC were seldom different among the treatments for either red maple or sugar maple, and the few times differences were detected, it was because trees in the Mid or Low treatments had higher concentrations relative to one or more of the other treatments—a pattern inconsistent with hypothesis H^1. Similarly, for wound closure, no treatment-related differences were found for red maple, and for sugar maple there was a tendency for trees in the Mid treatment to have slightly greater closure, which was inconsistent with H^2. Treatment differences in BAI per year also showed few significant patterns. For red maple, BAI growth in 2017 was significantly lower among trees in the High and Midx2 treatments relative to trees in the Low treatment, and in 2018, trees in all treatments had lower radial growth than trees in the Low treatment. Patterns more closely met a priori expectations (H^3) when the slopes of growth over time were evaluated and tested to see whether they showed signs of decline post treatment (slopes of the BAI growth over time regression lines being significantly less than zero). For red maple, there was no evidence of growth declines over time for trees in the Control or Low treatments, but significant and

Fig. 4. Basal area increment (BAI) growth relative to 5-year average growth before the first year of treatment (2016) for red maple trees from three crown injury classes: no injury, <50% injury, and ≥50% injury. The number of plots measured per treatment are noted. NS indicates that no statistical differences were detected. Error bars represent ±SE.

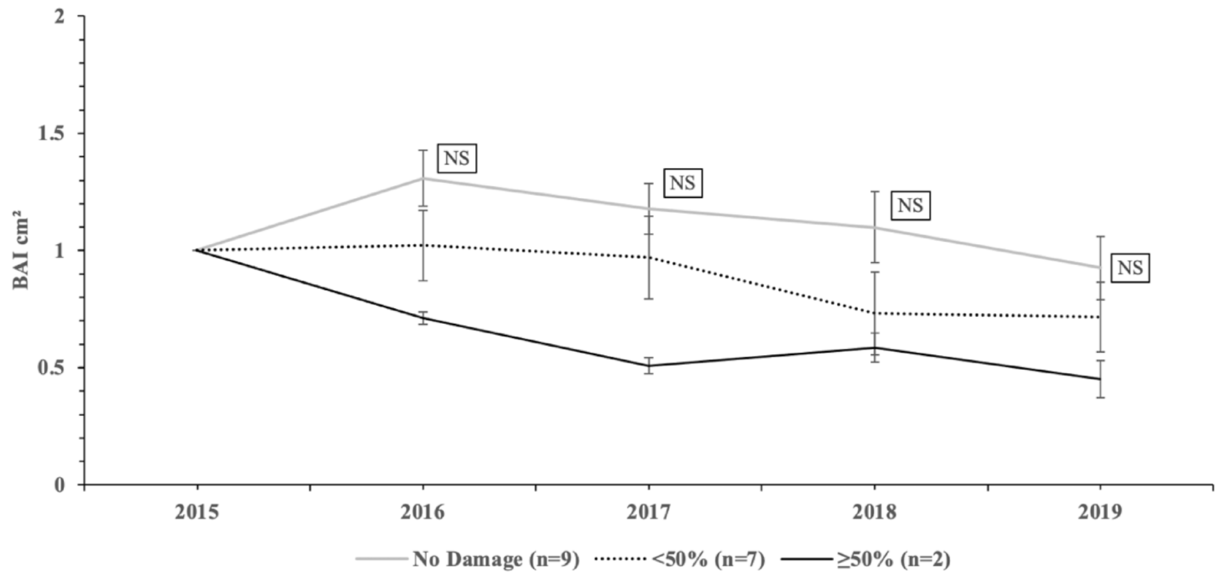

Fig. 5. Basal area increment (BAI) growth relative to 5-year average growth before the first year of treatment (2016) for sugar maple trees from three crown injury classes: no injury, <50% injury, and ≥50% injury. The number of plots measured per treatment are noted. NS indicates that no statistical differences were detected. Error bars represent ±SE.

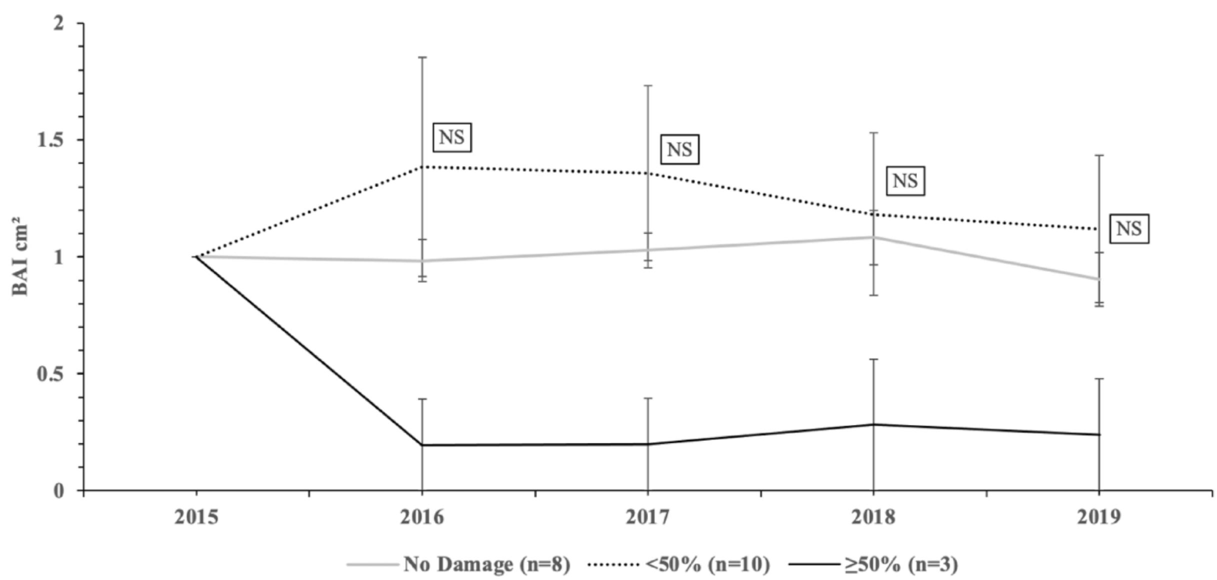

growing signs of decline as treatment intensities increased from Mid to Midx2 to High. For sugar maple, significant declines in BAI over time were only detected for trees in the High treatment.

Growth can also differ with tree size, with larger diameter trees being capable of greater BAI growth than smaller trees. There were small differences in DBH among ISE treatment groups, though these differences did not coincide with the few treatment differences detected. Red maple in the Mid treatment were smaller than those in the Control and High treatment ($P = 0.0088$). Yet trees in the Mid group grew no differently from trees in the High group, and growth of Control group trees was indistinguishable from growth of trees in all other treatments in half of the years assessed. Sugar maple trees in the Control and High groups were smaller than those in the Midx2 treatment ($P = 0.0005$). However, no differences in growth associated with treatment were found (Fig. 3), and slope analysis detected reductions in growth only for trees in the High treatment (Table 4).

Table 8. Analysis of regression line slopes over time by damage class—significance from zero as well as differences between damage classes for red maple and sugar maple trees.

Species	Damage class	N	Slope	Std. err.	Prob > *F* (Sig. from zero)	R^2
Red maple	No damage	9	− 0.0358	±0.0305	0.5305	0.1429
	<50%	7	− 0.0858	±0.0436	**0.0382**	0.8075
	≥50%	2	− 0.1222	±0.0194	**0.0447**	0.7872
	Prob > *F*	–	0.4370	–	–	–
Sugar maple	No damage	8	− 0.0095	±0.0297	0.7128	0.0518
	<50%	10	0.0036	±0.0666	0.9558	0.0012
	≥50%	3	− 0.1436	±0.0564	0.2304	0.4288
	Prob > *F*	–	0.3861	–	–	–

Crown damage class differences

Although ice accretion and resulting canopy damage generally met treatment expectations at the plot level (e.g., Campbell et al. 2020; Fahey et al. 2020), variations in crown damage among trees within plots was also evident (Rustad et al. 2020). Because physiological measurements were made on individual trees for which crown damage was visually assessed post treatment, we also evaluated how crown damage was related to NSC, wound closure, and BAI measurements across broad damage classes.

Even considering differences in crown damage classes among trees, few differences in NSC were detected. However, differences that were found met the expectation that higher crown damage would be associated with higher NSC concentrations (H^1). For red maple in 2017, concentrations of stachyose (a major storage and transport sugar in woody plants) were higher in trees with high crown damage relative to trees with lesser or no crown damage. For sugar maple in 2016, xylose (a structural sugar in the primary cell wall) was higher in trees with high crown damage relative to trees with lesser crown damage. Higher concentrations of NSC have been measured in the shoots of sugar maple trees with crown damage from the 1998 ice storm relative to undamaged trees (Wong et al. 2005). Higher concentrations may result from reduced use of NSC associated with declines in wound closure (Shortle et al. 2003) and growth (e.g., Lafon and Speer 2002; Smith and Shortle 2003; Pisaric et al. 2008) following extensive crown damage.

Accounting for the crown damage of individual trees also helped to detect more consistent differences in wound closure (H^2). For example, red maple with high crown damage experienced significantly less wound closure than red maple with less than 50% crown damage. For sugar maples, trees with no crown injury or moderate injury showed the greatest wound closure, whereas trees with high damage had less wound closure and trees that eventually died showing the least closure. Other work has documented reduced wound closure associated with progressively greater crown damage for both red maple and sugar maple (Shortle et al. 2003). Extensive crown damage results in the loss of carbon stores trapped within downed material and limits future carbon gains as leaf areas are reduced—two sources of energy (stored and newly produced carbohydrates) required to fuel wound repair.

ANOVA analyses showed no significant differences in BAI growth for red maple or sugar maple trees among the crown damage class categories. However, analyses of the slopes of regressions of BAI over time revealed significant reductions in growth for red maple trees in both the moderate and high crown damage classes—a pattern consistent with H^3. The slope of regressions of growth over time for sugar maples was not significant, indicating that any reductions in growth following crown damage were not linear. Nonetheless, orthogonal contrasts indicated that sugar maples with high crown damage experienced an approximately 80% reduction in radial growth the first growing season post treatment and remained at that low level thereafter. In comparison, red maple growth decreased by about 30% the first growing season post treatment, and growth continued to decline—eventually reaching an approximate 55% reduction by the end of the fourth-year post treatment. It appears that tree size did not influence differences in growth associated with crown damage because there were no differences in DBH among damage classes for red maple ($P = 0.1065$) or sugar maple ($P = 0.1950$).

It should also be noted that the physiological impacts that we detected for dominant and co-dominant sugar and red maples may differ from other species and crown classes. For example, although crown damage and loss were the typical response for high ice loading of large deciduous trees, crown damage was negligible for the few conifers on ISE plots. Furthermore, smaller pole-sized trees, especially American beech (*F. grandifolia*), experienced little crown damage but instead were sometimes dramatically bent over with little recovery of form after ice accumulations melted (Fahey et al. 2020; Rustad et al. 2020).

Species comparisons

Although some differential responses of red and sugar maple to ice damage were detected when evaluating treatment means for wound closure and BAI growth, differences in species response were more evident when crown damage classes were compared. As with treatment means, few differences in NSC associated with crown damage classes were found for either red or sugar maple trees. However, wound closure was reduced with greater crown damage for red maple, with sugar maple showing an even greater reduction in wound closure following crown loss (Table 7). This greater sensitivity of sugar maple to crown damage was even more evident with BAI growth. Red maple showed a gradual, linear decline in growth with crown loss (Table 8) reaching an approximately 55% reduction after 4 years (Fig. 4). In contrast, sugar maple growth decreased approximately 80% the first year following injury (Fig. 5). For comparison, Smith and Shortle (2003) found that crown loss of greater than one-half resulted in reduced radial growth of one-third to three quarters following the 1998 ice storm in New Hampshire and Maine. This study also reported that growth of sugar maple and red maple trees with extensive (>75%) crown loss was the lowest of the four species evaluated (Smith and Shortle 2003).

It has been hypothesized that sugar maple trees with extensive crown damage following ice storms preferentially allocate carbohydrates to rebuild their crowns instead of fully supporting radial growth (Pisaric et al. 2008). This response to extensive crown loss could promote tree survival in the long run but would result in low growth in the short-to-mid terms (Pisaric et al. 2008). Crown regrowth varies among species (Duguay et al. 2001), with sugar maple being a particularly good producer of sprouts that rebuild crowns post damage (Duguay et al. 2001; Pisaric et al. 2008). This capacity for crown regeneration may contribute to the perseverance of maples despite periodic damage from ice storms. *Acer* has been reported to have strong resilience and resistance to ice storms (Duguay et al. 2001; Shortle et al. 2003; Pisaric et al. 2008) and to be less susceptible to long-term decline relative to *Fagus* and *Tilia* (Deschênes et al. 2019) and several other genera (Pisaric et al. 2008). Considering this, the declines in wound closure and radial growth that we report may represent a short- to medium-term tradeoff relative to adaptations like enhanced crown recovery that support long-term survival.

We are uncertain whether sugar maple's greater sensitivity to the impacts of crown loss is related to the more generalized decline of this species, which has been attributed to acid deposition-induced calcium depletion (Driscoll et al. 2001; Schaberg et al. 2006). At Hubbard Brook, the decline of sugar maple trees started in the 1980s, while red maple trees appear to have been unimpacted (Fig. 1). Calcium depletion is thought to impair tree stress response physiology, which predisposes trees to decline following exposure to some other secondary stressor (e.g., drought, insect herbivory, etc.) (Schaberg et al. 2001). Addition of calcium to the forests of Hubbard Brook has been shown to reverse tree decline (Battles et al. 2014), improve wound closure, and increase BAI growth of sugar maple trees following ice storm damage (Huggett et al. 2007). The legacy of calcium depletion and tree decline at Hubbard Brook may itself be a contributing factor to the greater sensitivity of sugar maple to reduced growth and wound closure following crown damage in our study. Trees that are already in decline are more likely to respond poorly to further stress (e.g., Houston 1987; Pedersen 1998).

Acknowledgements

Funding for this research was provided by the National Science Foundation (DEB-1457675). We thank the many members of the ISE team who helped with the ice application and associated field and laboratory work, especially Geoff Schwaner, Gabe Winant, and Brendan Leonardi. This manuscript is a contribution of the Hubbard Brook Ecosystem Study. Hubbard Brook is part of the Long-Term Ecological Research (LTER) network, which is supported by the National Science Foundation (DEB-1637685). The HBEF is operated and maintained by the USDA Forest Service, Northern Research Station, Madison, WI.

Article information

History dates

Received: 5 August 2023
Accepted: 15 November 2023
Accepted manuscript online: 5 December 2023
Version of record online: 21 March 2024

Copyright

Data availability

The tree-ring datasets generated for this study will be available for download from The DendroEcological Network at https://www.uvm.edu/femc/dendro#data. Ice thickness data from the ISE are available from https://doi.org/10.6073/pasta/86d055125f1128290a637dcab45ae167.

Author information

Author ORCIDs

Paul G. Schaberg https://orcid.org/0000-0001-5936-2506
Christopher F. Hansen http://orcid.org/0000-0001-9333-3856
John L. Campbell https://orcid.org/0000-0003-4956-1696
Lindsey E. Rustad http://orcid.org/0000-0002-6683-2374

Author contributions

Conceptualization: PGS, JLC, LER
Data curation: CFH, PFM
Formal analysis: PGS, CFH, PFM
Funding acquisition: JLC, LER
Investigation: PGS, CFH, PFM, GJH, JLC
Project administration: PGS, GJH, JLC, LER
Supervision: PGS
Visualization: CFH, PFM
Writing – original draft: PGS
Writing – review & editing: CFH, PFM, GJH, JLC, LER

Competing interests

The authors declare there are no competing interests.

References

Battles, J.J., Fahey, T.J., Driscoll, C.T., Blum, J.D., and Johnson, C.E. 2014. Restoring soil calcium reverses forest decline. Environ. Sci. Technol. Lett. **1**(1): 15–19. doi:10.1021/ez400033d.

Bunn, A.G., Jansma, E., Korpela, M., Westfall, R.D., and Baldwin, J. 2013. Using simulations and data to evaluate mean sensitivity (f) as a useful statistic in dendrochronology. Dendrochronologia, **31**(3): 250–254. doi:10.1016/j.dendro.2013.01.004.

Campbell, J.L., Rustad, L.E., Driscoll, C.T., Halm, I., Fahey, T.J., Fakhraei, H., et al. 2020. Simulating impacts of ice storms on forest ecosystems. J. Vis. Exp. **160**: e61492.

Cheng, C.S., Li, G., and Auld, H. 2011. Possible impacts of climate change on freezing rain using downscaled future climate scenarios: updated for Eastern Canada. Atmosphere-Ocean, **49**(1): 8–21. doi:10.1080/07055900.2011.555728.

Cook, E.R., and Kairiukstis, L.A. 1990. Methods of dendrochronology. Kluwer Academic Publishers, Boston.

DeGaetano, A.T. 2000. Climatic perspective and impacts of the 1998 northern New York and New England ice storm. Bull. Am. Meteorol. Soc. **81**(2): 237–254. doi:10.1175/1520-0477(2000)081%3c0237:CPAIOT%3e2.3.CO;2.

Deschênes, É., Brice, M.H., and Brisson, J., 2019. Long-term impact of a major ice storm on tree mortality in an old-growth forest. For. Ecol. Manage. **448**: 386–394. doi:10.1016/j.foreco.2019.06.018.

Ding, Y., Jia, X., Wang, Z., Chen, X., and Chen, L. 2009. A contrasting study of freezing disasters in January 2008 and in winter of 1954/1955 in China. Front. Earth Sci. China, **3**(2): 129–145. doi:10.1007/s11707-009-0028-2.

Driscoll, C.T., Lawrence, G.B., Bulger, A.J., Butler, T.J., Cronan, C.S., Eagar, C., et al. 2001. Acidic deposition in the northeastern United States: sources and inputs, ecosystem effects, and management strategies: the effects of acidic deposition in the northeastern United States include the acidification of soil and water, which stresses terrestrial and aquatic biota. BioScience, **51**(3): 180–198.

Duguay, S.M., Arii, K., Hooper, M., and Lechowicz, M.J. 2001. Ice storm damage and early recovery in an old-growth forest. Environ. Monitor. Assess. **67**(1): 97–108. doi:10.1023/A:1006464511158.

Fahey, R.T., Atkins, J.W., Campbell, J.L., Rustad, L.E., Duffy, M., Driscoll, C.T., et al. 2020. Effects of an experimental ice storm on forest canopy structure. Can. J. For. Res. **50**: 136–145. doi:10.1139/cjfr-2019-0276.

Hooper, M.C., Arii, K., and Lechowicz, M.J. 2001. Impact of a major ice storm on an old-growth hardwood forest. Can. J. Bot. **79**: 70–75.

Houston, D.R. 1987. Forest tree declines of past and present: current understanding. Can. J. Plant Pathol. **9**(4): 349–360. doi:10.1080/07060668709501868.

Huggett, B.A., Schaberg, P.G., Hawley, G.J., and Eager, C. 2007. Long-term calcium addition increases growth release, wound closure, and health of sugar maple (*Acer saccharum*) trees at the Hubbard Brook Experimental Forest. Can. J. For. Res. **37**: 1692–1700. doi:10.1139/X07-042.

IPCC CC. Synthesis Report. 2014. Contribution of Working Groups I. II and III to the Fifth Assessment Report of the Intergovernmental Panel on Climate Change Core Writing Team. *Edited by* RK Pachauri and LA Meyer. IPCC, Geneva, Switzerland. p. 151.

Irland, L.C. 1998. Ice strom 1998 and the forests of the Northeast. J. For. **96**(9): 32–40.

Irland, L.C. 2000. Ice storms and forest impacts. Sci. Total Environ. **262**: 231–242. doi:10.1016/S0048-9697(00)00525-8.

Lafon, C.W., and Speer, J.H. 2002. Using dendrochronology to identify major ice storm events in oak forests of southwestern Virginia. Clim. Res. **20**(1): 41–54. doi:10.3354/cr020041.

Millward, A.A., and Kraft, C.E. 2004. Physical influences of landscape on a large-extent ecological disturbance: the northeastern North American ice storm of 1998. Landsc. Ecol. **19**: 99–111. doi:10.1023/B:LAND.0000018369.41798.2f.

Nagel, T.A., Firm, D., Rozenbergar, D., and Kobal, M. 2016. Patterns and drivers of ice storm damage in temperate forests of Central Europe. Eur. J. For. Res. **135**(3): 519–530. doi:10.1007/s10342-016-0950-2.

Pedersen, B.S. 1998. The role of stress in the mortality of midwestern oaks as indicated by growth prior to death. Ecology, **79**(1): 79–93. doi:10.1890/0012-9658(1998)079%5b0079:TROSIT%5d2.0.CO;2.

Pisaric, M.F., King, D.J., MacIntosh, A.J.M., and Bemrose, R. 2008. Impact of the 1998 ice storm on the health and growth of sugar maple (*Acer saccharum* Marsh.) dominated forests in Gatineau Quebec. J. Torrey Bot. Soc. **135**(4): 530–539. doi:10.3159/08-RA-053R.1.

Rhoads, A.G, Hamburg, S.P., Fahey, T.J., Siccama, T.G., Hane, E.N., Battles, J., et al. 2002. Effects of an intense ice storm on the structure of a northern hardwood forest. Can. J. For. Res. **32**: 1763–1775. doi:10.1139/x02-089.

Rustad, L.E., and Campbell, J.L. 2012. A novel ice storm manipulation experiment in a northern hardwood forest. Can. J. For. Res. **42**: 1810–1818. doi:10.1139/x2012-120.

Rustad, L.E., Campbell, J.L., Driscoll, C., Fahey, T.J., Groffman, P.M., Schaberg, P.G., et al. 2020. Experimental approach and initial forest response to a simulated ice strom experiment in a northern haardwood forest. PLoS ONE, **15**(9): e0239619. 25. doi:10.1371/journal.pone.0239619.

Schaberg, P.G., Dehayes, D.H., and Hawley, G.J. 2001. Anthropogenic calcium depletion: a unique threat to forest ecosystem health? Ecosys. Health, **7**: 214–228. doi:10.1046/j.1526-0992.2001.01046.x.

Schaberg, P.G., Tilley, J.W., Hawley, G.J., DeHayes, D.H., and Bailey, S.W. 2006. Associations of calcium and aluminum with the growth and health of sugar maple trees in Vermont. For. Ecol. Manage. **223**(1–3): 159–169. doi:10.1016/j.foreco.2005.10.067.

Shortle, W.C., Smith, K.T., and Dudzik, K.R. 2003. Tree survival and growth following ice storm injury. Res. Pap. NE-723. U.S. Department of Agriculture, Forest Service, Northeastern Research Station, Newtown Square, PA. 4 p.

Smith, K.T., and Shortle, W.C. 2003. Radial growth of hardwoods following the 1998 ice storm in New Hampshire and Maine. Can. J. For. Res. **33**(2): 325–329. doi:10.1139/x02-185.

Speer, J.H. 2010. Fundamentals of tree-ring research. The University of Arizona Press, Tucson.

Stokes, M., and Smiley, T. 1968. An introduction to tree-ring dating. University of Chicago Press., Chicago, IL. pp. 31–46.

Swaminathan, R., Sridharan, M., and Hayhoe, K.A. 2018. Computational framework for modelling and analyzing ice storms. arXiv eprints[internet]. Available from https://ui.adsabs.harvard.edu/abs/2018arXiv180504907S [accessed 1 May 2018].

Weitzman, J.N., Groffman, P.M., Campbell, J.L, Driscall, C.T., Fahey, R.T., Fahey, T.J., et al. 2020. Ecosystem nitrogen response to a simulated ice stron in a northern hardwood forest. Ecosystems, 1186–1205. doi:10.1007/s10021-019-00463-w.

Wuebbles, D., Meehl, G., Hayhoe, K., Karl, T.R., Kunkel, K., Santer, B., et al. 2014. CMIP5 climate model analyses: climate extremes in the United States. Bull. Am. Meteorol. Soc. **95**(4): 571–583. doi:10.1175/bams-d-12-00172.1.

Wong, B.L., Staats, L.J., Burfeind, A.S., Baggett, K.L., and Rye, A.H. 2005. Carbohydrate reserves in *Acer saccharum* trees damaged during the January 1998 ice strom in northern New York. Can. J. Bot. **83**: 668–677. doi:10.1139/b05-041.

Yamaguchi, D.K. 1991. A simple method for cross-dating increment cores from living trees. Can. J. For. Res. **21**(3): 414–416. doi:10.1139/x91-053.